Acta Biochim Biophys Sin 2013, 45: 720–725 | © The Author 2013. Published by ABBS Editorial Office in association with Oxford University Press on behalf of the Institute of Biochemistry and Cell Biology, Shanghai Institutes for Biological Sciences, Chinese Academy of Sciences. DOI: 10.1093/abbs/gmt066.
Advance Access Publication 16 June 2013

Original Article

The crystal structure of human GDP-L-fucose synthase

Huan Zhou[1], Lihua Sun[1], Jian Li[1], Chunyan Xu[1], Feng Yu[1], Yahui Liu[1], Chaoneng Ji[2], and Jianhua He[1*]

[1]Department of Biological Sciences, Shanghai Institute of Applied Physics, Chinese Academy of Sciences, Shanghai 201204, China
[2]State Key Laboratory of Genetic Engineering, Institute of Genetics, School of Life Sciences, Fudan University, Shanghai 200433, China
*Correspondence address. Tel: +86-21-33933186; Fax: +86-21-33933021; E-mail: hejh@sinap.ac.cn

Human GDP-L-fucose synthase, also known as FX protein, synthesizes GDP-L-fucose from its substrate GDP-4-keto-6-deoxy-D-mannose. The reaction involves epimerization at both C-3 and C-5 followed by an NADPH-dependent reduction of the carbonyl at C-4. In this paper, the first crystal structure of human FX protein was determined at 2.37 Å resolution. The asymmetric unit of the crystal structure contains four molecules which form two homodimers. Each molecule consists of two domains, a Rossmann-fold NADPH-binding motif and a carboxyl terminal domain. Compared with the *Escherichia coli* GDP-L-fucose synthase, the overall structures of these two enzymes have four major differences. There are four loops in the structure of human FX protein corresponding to two α-helices and two β-sheets in that of the *E. coli* enzyme. Besides, there are seven different amino acid residues binding with NAPDH comparing human FX protein with that from *E. coli*. The structure of human FX reveals the key catalytic residues and could be useful for the design of drugs for the treatment of inflammation, autoimmune diseases, and possibly certain types of cancer.

Keywords gdp-L-fucose synthase; gdp-L-fucose; fx

Received: February 2, 2013 Accepted: March 27, 2013

Introduction

In mammals, fucosylated glycans play important roles in ABO blood group antigens, host–microbe interactions, and several human diseases, such as rheumatoid arthritis, pancreatic cancer, hepatocellular carcinoma, gastrointestinal cancer, and a rare congenital disease LAD II (leukocyte adhesion deficiency II, also known as congenital disorder of glycosylation IIc, CDG IIc) [1–5].

All fucosylated oligosaccharides are constructed by fucosyltransferases with the only fucose donor, GDP-L-fucose [6]. There are two GDP-L-fucose synthesis pathways in the cytosol—the salvage pathway and the *de novo* pathway [6]. The former pathway synthesizes GDP-L-fucose from free L-fucose via two steps involving L-fucokinase and GDP-L-fucose pyrophosphorylase [7,8]. The later pathway converts GDP-D-mannose to GDP-L-fucose via three enzymatic reactions, which are catalyzed by GDP-D-mannose 4, 6-dehydratase (GMD) and GDP-4-keto-6-deoxy-D-mannose-3, 5-epimerase-4-reductase (FX) [9,10]. FX-knockout mice exhibit a complete deficiency of cellular fucosylation, which indicates that the *de novo* pathway is the major route for cellular GDP-L-fucose biosynthesis *in vivo* [11].

FX was first isolated from human erythrocytes in 1976 and recognized as an NADPH-binding protein [12]. It has been known for several years that the enzyme is responsible for the last step of the major metabolic pathway synthesizing GDP-L-fucose from GDP-D-mannose in prokaryotes and eukaryotes [10]. Recently, it has been found that the expression of FX enzyme in head and neck squamous carcinoma cells was up-regulated by the glycosyl-phosphatidylinositol-linked Ly-6 antigen E48 [13]. FX is also regulated by outside-in signals in lymphocytes and it may take part in the cascade of events leading to the extravasation of activated lymphocytes [14]. The expression of FX also increases by 70% in human hepatocellular carcinoma (HCC) tissues, compared with the adjacent non-tumor tissues and normal livers, thus the elevation in GDP-L-fucose levels and the up-regulation of FX expression represent potential markers for HCC [15].

The 3D structure of FX from *Escherichia coli* was determined by two research groups simultaneously and was confirmed belonging to the short-chain dehydrogenases/reductases family (SDR) which has a highly conserved TyrXXXLys catalytic couple [16,17]. In this family, some structures of the other related enzymes are known, such as UDP-galactose 4-epimerase (UGE), which catalyzes the interconversion of UDP-galactose and UDP-glucose, and GMD, which catalyzes the conversion of GDP-D-mannose to GDP-4-keto-6-deoxy-D-mannose [18–28].

Materials and Methods

Protein expression and purification

The *fx* gene was cloned into a pET28b vector with an N-terminal $(His)_6$ fusion tag, and transformed into *E. coli*

expression strain BL21(DE3). A glycerol stock of culture was used to inoculate a starter culture, 100 ml of Luria–Bertani (LB) media. After cultivation overnight at 37°C, the starter culture was transferred into 1 l of LB media. When OD_{600} reached ~0.6, the temperature was set to 25°C and then the protein expression was induced by 1 mM isopropyl-β-galactoside, and the cells were left to grow overnight. Cells were harvested by centrifugation and the pellets were stored at −80°C until processed. In the experiment, the pellets were resuspended in buffer A (20 mM Tri-HCl, pH 8.0, 300 mM NaCl, 5 mM imidazole). French press was employed to lyse the cells, and then the sample was centrifuged at 16,000 rpm and 4°C for 30 min, the supernatant was collected, and the cell debris was discarded. The supernatant was loaded onto a column of 5 ml Ni-nitrilotriacetic acid resin. The column was washed with buffer A (20 mM Tri-HCl, pH 8.0, 300 mM NaCl, 5 mM imidazole), and protein was eluted with buffer B (20 mM Tri-HCl, pH 8.0, 300 mM NaCl, 300 mM imidazole). Further purification was carried out by Fast protein liquid chromatography using gel filtration on a Superdex 200 16/60 column (GE Healthcare, Uppsala, Sweden) equilibrated with 20 mM Tri-HCl (pH 8.0) containing 100 mM NaCl. The peak fractions were pooled and concentrated to 20 mg/ml for crystallization.

Crystallization

Before crystallization, NADPH was added into the purified FX to the final concentration of 5 mM. Crystallization was carried out by using the hanging drop vapor diffusion method. Crystals suitable for X-ray experiment were grown after microseeding in a drop containing equal amounts of protein and well solution (100 mM Tris, pH 8.0, 30% polyethylene glycol monomethyl ether 2000).

X-ray data collection and processing

Crystals were mounted in cryoloops with respective reservoir solution containing 25% glycerol for 1 min and then flash-frozen in liquid nitrogen. Data collection was performed at 100 K on beamline BL17U at the Shanghai Synchrotron Radiation Facility (Shanghai, China). X-ray diffraction data were recorded using an ADSC Q315 detector positioned at a distance of 250 mm from the crystal. A total of 180 frames of diffraction images were taken with 1° oscillation steps and 1 s exposure per frame. Bragg reflections were processed to 2.37 Å resolution using HKL2000 [29]. Data collection statistics are presented in **Table 1**.

Structure determination and refinement

The structure of FX was determined by molecular replacement by AMoRe from the CCP4 suite using the structure of FX from *E. coli* [17] as a search model. The human GDP-L-fucose synthase crystal belongs to space group $P2_12_12_1$, and the detailed crystallographic data statistics are shown in **Table 1**.With a dimer as a search model, clear solutions for two dimers were obtained. Several rounds of manual inspection and rebuilding using Coot [30] were performed. The PHENIX suite [31] was then employed for final rounds of refinement. The model was refined to a final R_{work} of 23.21% and an R_{free} of 28.97%. The refinement statistics are outlined in **Table 1**.

Results

Overall structure

For the structure determined in this study, each asymmetric unit contains 4 protein molecules, 4 NADPH molecules, and 23 water molecules. Certain areas of the protein are missing in the structures: missing residues 1–6, 33–35, and 237–277 in chain A, missing residues 1–6, 33–35, 204, 268,

Table 1 Crystal data collection and structure-refinement statistics

Data collection Space group	$P2_12_12_1$
Cell dimensions	
a, b, c (Å)	85.26, 136.26, 139.52
Resolution (Å)	2.37 (2.41–2.37)
R_{merge} [a]	0.118 (0.863)
$I/\sigma I$	80.6 (4.2)
Completeness (%)	100.0 (100.0)
Redundancy	7.6 (7.5)
Refinement	
Resolution range	39.27–2.37
Reflections in working set	67,223
Reflections in test set	4864
R_{work} [b], R_{free} [c]	23.21, 28.97
Number of non-H atoms	
Protein atoms	9955
NADPH	4
Water	23
Mean temperature factor, Å^2	39.9
Rmsd	
Bond lengths, Å	0.009
Bond angles, °	1.373
Ramachandran plot	
Favored (%)	88.4%
Allowed (%)	7.9%
Outliers (%)	3.8%
PDB code	4E5Y

Values in parentheses are for the highest resolution shell.

[a] $R_{merge} = \Sigma_{hkl}\Sigma_i|I_i(hkl) - \langle I(hkl)\rangle|/\Sigma_{hkl}\Sigma_i I_i(hkl)$ where $\langle I(hkl)\rangle$ is the mean intensity of a set of equivalent reflections.

[b] $R_{work} = \Sigma_{hkl}||F_{obs}| - |F_{calc}||/\Sigma_{hkl}|F_{obs}|$, where F_{obs} and F_{calc} are observed and calculated structure factors, respectively.

[c] R_{free} is the same as R_{merge} except that it was calculated for a randomly chosen 5% test set that was excluded from refinement.

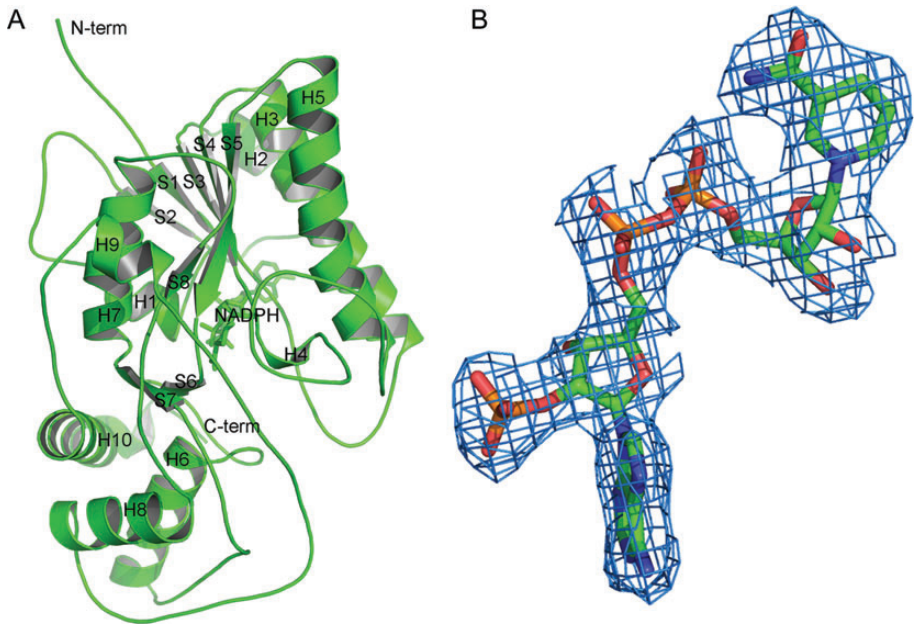

Figure 1 The overall fold of FX (A) A stereo ribbon-cartoon drawing of the FX monomer. The secondary structure elements are labeled proceeding from N to C terminus. The NADPH cofactor is shown in stick representation. (B) A Fo-Fc OMIT map of NADPH is shown in stereo at a contour level of 1.0 sigma. The map was calculated by excluding NADPH from the model using CNS.

and 278 in chain B, missing residues 1–6, 33–35, 73–80, 194–201, and 264–271 in chain C, and missing residues 1–3 in chain D.

The ribbon representation of the FX monomer is displayed in **Fig. 1**. As a member of the NDP-sugar-modified SDR subfamily, the FX molecule folds into two domains: the N-terminal cofactor-binding domain and the C-terminal substrate-binding domain. The N-terminal domain is the predominant part of FX and includes amino acid residues 1–170, 220–242, and 287–292; and a smaller C-terminal domain includes amino acid residues 172–219, 252–263, and 301–321. The N-terminal domain consists of a Rossmann-fold motif, which commonly exists in SDR family enzymes, and the central β-strand consists of six-stranded parallel β-strands (S1–S5, S8), flanked by seven α-helices (H2–H5 on one side and H1, H7, and H9 on the other side). This domain is associated with the tight binding of the enzymatic cofactor NADPH. The C-terminal domain is a globular cluster of two small parallel β-strands (S6 and S7) and three α-helices (H6, H8, and H10), which are responsible for binding the substrate GDP-4-keto-6-deoxy-D-mannose.

The overall structure of human FX and that of the FX from *E. coli* can be superimposed well on each other, and the root mean square deviation is only 1.6 Å (319/318 residues) (**Fig. 2**), despite an overall sequence identity of only 28% between these two enzymes [17]. Although most of the secondary structural elements of these two proteins are very similar, there are also some differences. In the *E. coli* FX, there are two more insertions of α-helices in the N-terminal domain, consisting of residues 69–74 and 229–325, and there are two additional insertions of β-sheet in the C-terminal domain, consisting of residues 198–202 and 269–273, which are all missing in the human FX.

Quaternary structure and inter-molecular contacts

Human FX is found as a homodimer in solution, which is checked by gel filtration (data not shown). In the crystal, the asymmetric unit contains two separate crystallographic dimers (**Fig. 3**) and each dimer has an extensive inter-molecular interface. The core of the inter-molecular interface is formed by a four-helix bundle, which is composed of the most extended helices in each monomer (H3 and H5). Multimerization through a four-helix-bundle motif is a common feature in the SDR family.

NADPH-binding site

The electron density corresponding to NADPH is well defined in each subunit (**Fig. 1**). Consistent with previous homologous structures, the NADPH cofactor binds in an extended conformation and the average distance between the adenine C6 and the nicotinamide C2 position is 15.0 Å. A close-up view of the active site is shown in **Fig. 4**. Potential hydrogen bonding interactions between the protein and NADPH are indicated by dashed lines.

The adenine ring packs between the side chains of Asp47, Leu48, and a water molecule. N6 of the adenine base forms hydrogen bond with the side chain of Asp47. N1 is hydrogen-bonded to Leu48 peptidic N. N3 interacts with a water molecule. The adenosine ribose 2′-phosphate O2X is hydrogen-bonded to Ser43 peptidic N and Ser42 OG atom, and O2B is hydrogen-bonded to Ser16 OG atom. The

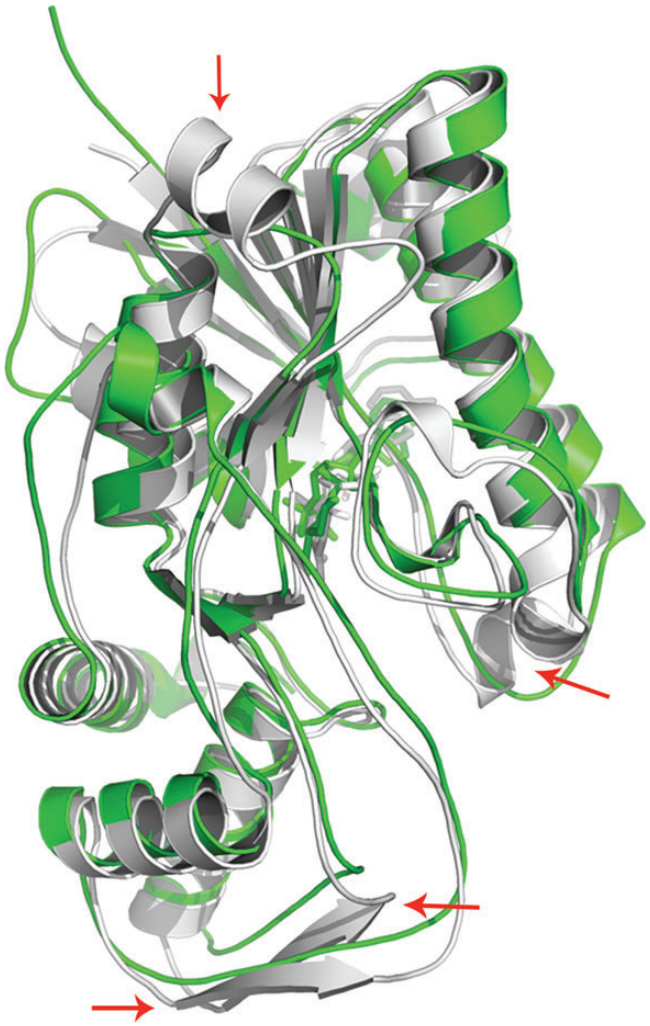

Figure 2 Superposition of the structure of *Homo sapiens* FX (green) and *E. coli* FX (white) (PDB ID: 1BSV) Red arrows indicate the differences between these two structures.

puckered ribose ring is hydrogen-bonded at the 3′-OH to the peptidic N atom of residue Ser16.

The dinucleotide diphosphate bridge is located next to residues Gly14−Gly20 that are provided by a loop comprising the sequence motif Gly14-X-X-Gly17-X-X-Gly20. The Gly-X-X-Gly-X-X-Gly motif is strongly conserved in *E. coli* FX, UGE, and related enzymes in the SDR family [16,17,21]. O1A is hydrogen-bonded to the Arg320 NH2 atom; O2A is hydrogen-bonded to the Arg320 NH1 atom and the Leu18 peptidic N atom, respectively; and O2N is hydrogen-bonded to the peptidic N atoms of residues Leu18 and Val19.

The nicotinic ribose ring is strongly hydrogen-bonded to protein residues. 2′-OH group is hydrogen-bonded to Tyr143 OH atom and Lys147 NZ atom. 3′-OH is hydrogen-bonded to Lys147 NZ atom and Leu69 carbonyl O atom. The hydrogen bonding of the nicotinic ribose hydroxyls by Lys and Tyr is highly conserved among related enzymes. The nicotinamide ring is bound in the *syn* conformation and may be stabilized in this orientation by hydrogen bonding to the residue Val173 peptidic N atom. This conformation is consistent with those of other SDR enzymes, allowing a B-side hydride transfer during catalysis.

Discussion

The proposed catalytic mechanism for FX occurs via a three-step process [32]. The first step involves a deprotonation at C-3 of GDP-D-mannose to yield an enolate intermediate, which is reprotonated on the opposite side to form GDP-6-deoxy-4-keto-altrose. The second step involves a similar deprotonation/reprotonation reaction that converts

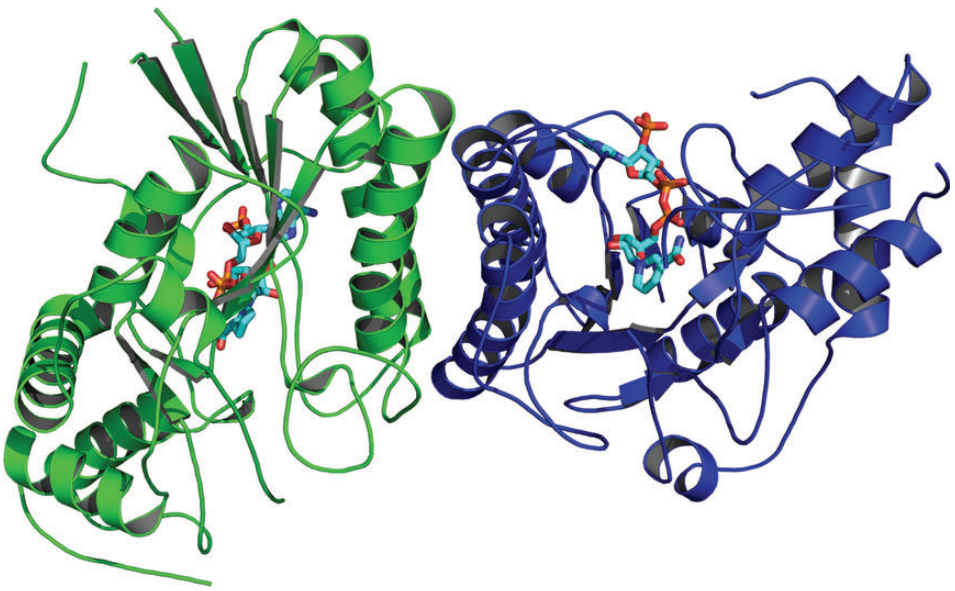

Figure 3 Ribbon representation of the FX dimer.

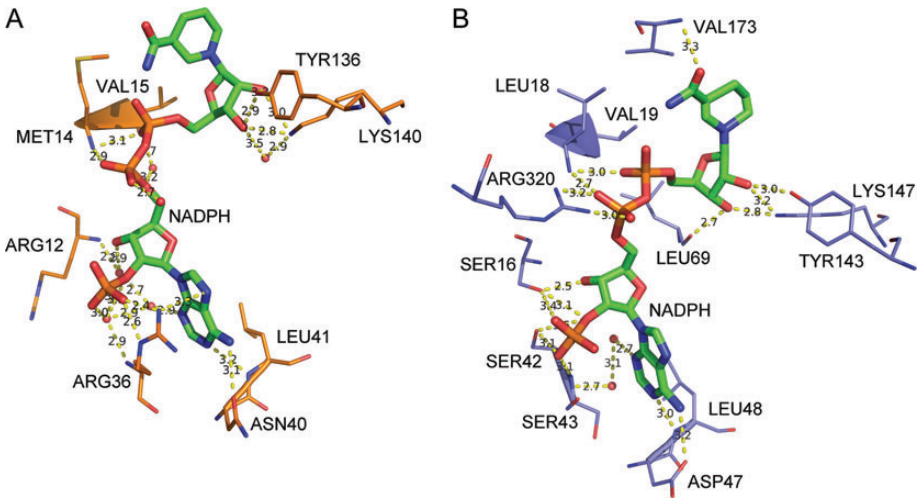

Figure 4 The NADPH-binding site (A) Stereoview of NADPH-binding interactions in FX from *H. sapiens*. Protein residues (stick model) and waters (red balls) involving in binding NADPH are shown. (B) Stereoview of NADPH-binding interactions in FX from *E. coli*. Protein residues (stick model) and waters (red balls) involving in binding NADPH are shown (PDB ID: 1BSV).

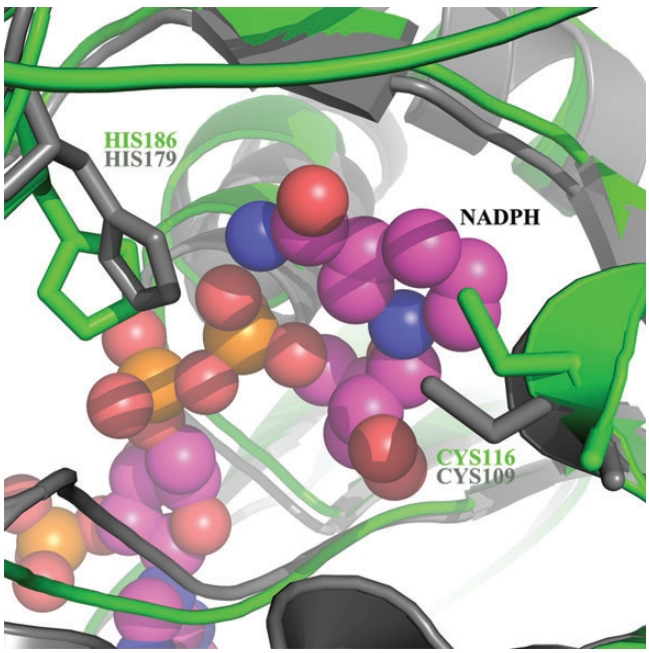

Figure 5 Superposition of the active sites position of *H. sapiens* FX (green) and *E. coli* FX (gray) (PDB ID: 1BSV).

the stereochemistry at C-5 of GDP-6-deoxy-4-keto-altrose to form GDP-6-deoxy-4-keto-L-galactose. Finally, an NADPH-dependent reduction converts the C-4 ketone into a hydroxyl group and produces GDP-L-fucose.

Lau and Tanner [32] demonstrated that Cys109 and His179 act as a base and an acid, respectively, in both epimerization reactions, which are catalyzed by *E. coli* FX. Comparing the molecular structure of human FX with that of *E. coli* FX, the spatial positions of Cys116 and His186 in human FX are the same as the spatial positions of Cys109 and His179 in *E. coli* FX (**Fig. 5**). Based on the similarity of two structures, we conclude that Cys116 and His186 play a similar role in human enzyme, as Cys109 and His179 behave in *E. coli* FX. It reveals the key catalytic residues in human FX and could be useful for the design of drugs for the treatment of inflammation, auto-immune diseases, and possibly certain types of cancer.

Acknowledgements

We would like to thank Dr Thomas Earnest for reading and revising this paper.

Funding

This work was supported by grants from the Ministry of Science and Technology of China (No. 2011CB911102) and the National Natural Science Foundation of China (No. 31100528).

References

1 Becker DJ and Lowe JB. Fucose: biosynthesis and biological function in mammals. Glycobiology 2003, 13: 41R–53R.
2 Okuyama N, Ide Y, Nakano M, Nakagawa T, Yamanaka K, Moriwaki K and Murata K, *et al*. Fucosylated haptoglobin is a novel marker for pancreatic cancer: a detailed analysis of the oligosaccharide structure and a possible mechanism for fucosylation. Int J Cancer 2006, 118: 2803–2808.
3 Ang IL, Poon TCW, Lai PBS, Chan ATC, Ngai SM, Hui AY and Johnson PJ, *et al*. Study of serum haptoglobin and its glycoforms in the diagnosis of hepatocellular carcinoma: a glycoproteomic approach. J Proteome Res 2006, 5: 2691–2700.
4 Moriwaki K and Miyoshi E. Fucosylation and gastrointestinal cancer. World J Hepatol 2010, 2: 151–161.
5 Yakubenia S and Wild MK. Leukocyte adhesion deficiency II advances and open questions. FEBS J 2006, 273: 4390–4398.
6 Ma B, Simala-Grant JL and Taylor DE. Fucosylation in prokaryotes and eukaryotes. Glycobiology 2006, 16: 158R–184R.

7 Park SH, Pastuszak I, Drake R and Elbein AD. Purification to apparent homogeneity and properties of pig kidney L-fucose kinase. J Biol Chem 1998, 273: 5685–5691.

8 Pastuszak I, Ketchum C, Hermanson G, Sjoberg EJ, Drake R and Elbein AD. GDP-L-fucose pyrophosphorylase. Purification, cDNA cloning, and properties of the enzyme. J Biol Chem 1998, 273: 30165–30174.

9 Sullivan FX, Kumar R, Kriz R, Stahl M, Xu GY, Rouse J and Chang XJ, *et al*. Molecular cloning of human GDP-mannose 4,6-dehydratase and reconstitution of GDP-fucose biosynthesis in vitro. J Biol Chem 1998, 273: 8193–8202.

10 Tonetti M, Sturla L, Bisso A, Benatti U and De Flora A. Synthesis of GDP-L-fucose by the human FX protein. J Biol Chem 1996, 273: 27274–27279.

11 Smith PL, Myers JT, Rogers CE, Zhou L, Petryniak B, Becker DJ and Homeister JW, *et al*. Conditional control of selectin ligand expression and global fucosylation events in mice with a targeted mutation at the FX locus. J Cell Biol 2002, 158: 801–815.

12 Morelli A and Flora DA. Isolation and partial characterization of an NADP and NADPH binding protein from human erythrocytes. Arch Biochem Biophys 1977, 179: 698–705.

13 Eshel R, Zanin A, Sagi-Assif O, Meshel T, Smorodinsky NI, Dwir O and Alon R, *et al*. The GPI-linked Ly-6 antigen E48 regulates expression levels of the FX enzyme and of E-selectin ligands on head and neck squamous carcinoma cells. J Biol Chem 2000, 275: 12833–12840.

14 Eshel R, Besser M, Zanin A, Sagi-Assif O and Witz IP. The FX enzyme is a functional component of lymphocyte activation. Cell Immunol 2001, 213: 141–148.

15 Noda K, Miyoshi E, Gu J, Gao CX, Nakahara S, Kitada T and Honke K, *et al*. Relationship between elevated FX expression and increased production of GDP-L-fucose, a common donor substrate for fucosylation in human hepatocellular carcinoma and hepatoma cell lines. Cancer Res 2003, 63: 6282–6289.

16 Rizzi M, Tonetti M, Vigevani P, Sturla L, Bisso A, Flora AD and Bordo D, *et al*. GDP-4-keto-6-deoxy-D-mannose epimerase/reductase from *Escherichia coli*, a key enzyme in the biosynthesis of GDP-L-fucose, displays the structural characteristics of the RED protein homology superfamily. Structure 1998, 6: 1453–1465.

17 Somers WS, Stahl ML and Sullivan FX. GDP-fucose synthetase from *Escherichia coli*: structure of a unique member of the short-chain dehydrogenase/reductase family that catalyzes two distinct reactions at the same active site. Structure 1998, 6: 1601–1612.

18 Bauer AJ, Rayment I, Frey PA and Holden HM. The molecular structure of UDP-galactose 4-epimerase from *Escherichia coli* determined at 2.5 Å resolution. Proteins 1992, 12: 372–381.

19 Thoden JB, Frey PA and Holden HM. Crystal structures of the oxidized and reduced forms of UDP-galactose 4-epimerase isolated from *Escherichia coli*. Biochemistry 1996, 35: 2557–2566.

20 Thoden JB, Hegeman AD, Wesenberg G, Chapeau MC, Frey PA and Holden HM. Structural analysis of UDP-sugar binding to UDP-galactose 4-epimerase from *Escherichia coli*. Biochemistry 1997, 36: 6294–6304.

21 Thoden JB, Wohlers TM, Fridovich-Keil JL and Holden HM. Crystallographic evidence for Tyr 157 functioning as the active site base in human UDP-galactose 4-epimerase. Biochemistry 2000, 39: 5691–5701.

22 Shaw MP, Bond CS, Roper JR, Gourley DG, Ferguson MA and Hunter WN. High-resolution crystal structure of *Trypanosoma brucei* UDP-galactose 4-epimerase: a potential target for structure-based development of novel trypanocides. Mol Biochem Parasitol 2003, 126: 173–180.

23 Thoden JB and Holden HM. The molecular architecture of galactose mutarotase/UDP-galactose 4-epimerase from *Saccharomyces cerevisiae*. J Biol Chem 2005, 280: 21900–21907.

24 Sakuraba H, Kawai T, Yoneda K and Ohshima T. Crystal structure of UDP-galactose 4-epimerase from the hyperthermophilic archaeon *Pyrobaculum calidifontis*. Arch Biochem Biophys 2011, 512: 126–134.

25 Somoza JR, Menon S, Schmidt H, Joseph-McCarthy D, Dessen A, Stahl ML and Somers WS, *et al*. Structural and kinetic analysis of *Escherichia coli* GDP-mannose 4, 6 dehydratase provides insights into the enzyme's catalytic mechanism and regulation by GDP-fucose. Structure 2000, 8: 123–135.

26 Mulichak AM, Bonin CP, Reiter WD and Garavito RM. Structure of the MUR1 GDP-mannose 4, 6-dehydratase from *Arabidopsis thaliana*: implications for ligand binding and specificity. Biochemistry 2002, 41: 15578–15589.

27 Webb NA, Mulichak AM, Lam JS, Rocchetta HL and Garavito RM. Crystal structure of a tetrameric GDP-D-mannose 4, 6-dehydratase from a bacterial GDP-D-rhamnose biosynthetic pathway. Protein Sci 2004, 13: 529–539.

28 Rosano C, Zuccotti S, Sturla L, Fruscione F, Tonetti M and Bolognesi M. Quaternary assembly and crystal structure of GDP-D-mannose 4,6 dehydratase from *Paramecium bursaria* Chlorella virus. Biochem Biophys Res Commun 2006, 339: 191–195.

29 Otwinowski Z and Minor W. Methods in enzymology. New York: Academic Press, 1999.

30 Emsley P and Cowtan K. Coot: model-building tools for molecular graphics. Acta Crystallogr D Biol Crystallogr 2004, 60: 2126–2132.

31 Adams PD, Grosse-Kunstleve RW, Hung LW, Ioerger TR, McCoy AJ, Moriarty NW and Read RJ, *et al*. PHENIX: building new software for automated crystallographic structure determination. Acta Crystallogr D Biol Crystallogr 2002, 58: 1948–1954.

32 Lau ST and Tanner ME. Mechanism and active site residues of GDP-fucose synthase. J Am Chem Soc 2008, 130: 17593–17602.